

# Ferromagnetism in Insulating, Doped Diluted Magnetic Semiconductors

Xin Wan and R. N. Bhatt

*Department of Electrical Engineering, Princeton University, Princeton, NJ 08544-5263*

(April 29, 2024)

We report results of a Monte Carlo study of doped, diluted magnetic semiconductors in the low carrier density (insulating) regime. We find that the system undergoes a transition from a paramagnet at high temperatures to a ferromagnet at low temperatures. However, in strong contrast to uniform systems, disorder effects dominate the entire collective behavior, leading to very unconventional properties such as (1) magnetization curves that cannot be described by theories based on critical fluctuations, or on spin wave analysis over any significant fraction of the phase diagram; (2) a large peak in susceptibility well below the ordering temperature; and (3) specific heat curves that point out the inadequacy of a classical Heisenberg model for spin-5/2 Mn ions. A picture of percolating magnetic polarons appears to describe the data well, and leads to a prescription for correcting the unphysical results of the classical continuous spin model in terms of a discrete vector model.

In diluted magnetic semiconductors (DMS), such as  $\text{Zn}_{1-x}\text{Mn}_x\text{Te}$  and  $\text{Cd}_{1-x}\text{Mn}_x\text{Se}$ , carriers localized at impurities can induce sizable magnetic moments on the scale of their hydrogen-like orbits. These entities, known as bound magnetic polarons (BMPs), are created by the  $sp-d$  exchange interactions of localized carriers with magnetic ions in their vicinity. The mechanism and thermodynamics of mutually independent BMPs in lightly doped DMS are well understood [1,2]. However, experiments on doped, p-type  $\text{ZnMnTe}$  [3] at intermediate doping densities (but clearly below the transition to a metallic state), have shown a significant enhancement in susceptibility at low temperatures ( $T$ ), implying a weak ferromagnetic polaron-polaron interaction. Based on an idealized, but exactly solvable, model of the single polaron, Wolff *et al.* [4] concluded that  $\text{Mn}^{2+}$  spins in the intervening region between polarons formed around two bound carriers can generate an effective ferromagnetic interaction between the two polarons which likely overcomes the direct antiferromagnetic interactions between impurities (due to virtual carrier hopping, as in usual nonmagnetic semiconductors).

In this paper, we report a Monte Carlo study of a more realistic model (with spatially dependent carrier wavefunctions) and demonstrate the generation of such effective ferromagnetic interactions within a model with only antiferromagnetic exchange interactions. We find that the system undergoes a transition to a ferromagnetic state below  $T = T_c$ ; however, the state is characterized by a very inhomogeneous spatial magnetization pattern, with a large (but finite) peak in the magnetic susceptibility at a temperature  $T_p$  well (one or two decades) below  $T_c$ , and  $T_p/T_c$  can be tuned, depending on the carrier density. Furthermore, the classical (continuous spin) Heisenberg model is found to yield unphysical results for the low-T specific heat, which is corrected by using a discrete vector spin model.

The  $sp-d$  exchange interaction of a localized carrier with a magnetic ion on a distance  $\mathbf{R}$  can be described by the spin Hamiltonian:

$$\mathcal{H} = J_0 |\phi(\mathbf{R})|^2 \mathbf{s} \cdot \mathbf{S}, \quad (1)$$

where  $J_0$  is the exchange constant, while  $\mathbf{s}$  and  $\mathbf{S}$  are spins of the carrier and the magnetic ion, respectively. For this study, we consider for concreteness the case of electron doping ( $s = 1/2$ ); our qualitative results are, however, valid for both electron and hole doping. The orbital wavefunction of the localized carrier  $\phi(r)$  is taken to be of a hydrogenic form  $\phi(r) = e^{-r/a_B}$  for simplicity in which  $a_B$  is the Bohr radius of the hydrogen-like orbit; extending to other spatial forms is straightforward.

On a zincblende lattice, Mn ions are introduced randomly to replace cations (one of the two interpenetrating fcc lattices) while the dopants replace anions randomly on the other sublattice. The ratio of Mn ions to dopants is taken to be 32:1, which corresponds roughly to 0.1% Mn at a doping concentration of  $10^{18} \text{cm}^{-3}$ . The Bohr radius  $a_B$  is taken at a typical value of  $20\text{\AA}$  and the lattice constant  $a_0 = 5\text{\AA}$ . Following Wolff *et al.* [4], the direct coupling between carrier spins has been neglected. In fact, we have found that introducing such a coupling at the densities studied has no qualitative effects on the thermodynamic phase diagram, and very minor quantitative changes. We also exclude direct Mn-Mn interactions among 0.1% substitutional manganese ions, since only 1% of these Mn ions have nearest neighbors. (The main effect of these pairs or larger clusters is to effectively reduce the percentage of active Mn spins, since most cluster interactions reduce the net magnetic moment - e.g. pairs form inert singlets). The Hamiltonian can be written as

$$\mathcal{H} = \sum_{i,j} J(\mathbf{r}_i, \mathbf{R}_j) \mathbf{s}_i \cdot \mathbf{S}_j, \quad (2)$$

where  $\mathbf{r}_i$  and  $\mathbf{s}_i$  are position and spin of the  $i$ -th carrier spin, while  $\mathbf{R}_j$  and  $\mathbf{S}_j$  those of the  $j$ -th Mn spin. All the spins are treated as classical Heisenberg spins. The exchange between a Mn spin and a carrier spin is given by,

$$J(\mathbf{r}_i, \mathbf{R}_j) = J_0 e^{-2|\mathbf{r}_i - \mathbf{R}_j|/a_B}. \quad (3)$$

We carried out simulations on lattices of linear size  $L = 40$  to  $80$ , which contain  $N_c = 8$  to  $64$  dopants and  $N_d = 256$  to  $2048$  Mn ions. We averaged up to  $3000$  samples per data point, depending on  $L$  and  $T$ .  $J_0$  is taken as the unit of  $T$ . The equilibration of each system, which consists of as many as  $2048$  Mn spins, is checked by the following technique. We simulate two mutually independent samples with identical locations of particles but different initial spin configurations. One sample starts from totally random spin configuration, while the other from an ordered state, where the electron spins and the Mn spins are oriented ferromagnetically within each kind but opposite to the other kind. The evolutions of the two samples correspond to the relaxations from high  $T$  and low  $T$  limit respectively. We expect to obtain the same results, such as magnetization and energy, in both samples for sufficient long time  $t$ , when equilibrium is reached.

Figure 1 shows the evolution of average magnetization  $\langle |M| \rangle$  with  $t$  for  $256$  Mn spins and temperature  $T = 0.01$ . From the convergence of the two curves we can determine the equilibration time for that  $L$  and  $T$ . Because the magnetization values in the two replicas approach the equilibrium from different directions, we are able to obtain the equilibrium results to desired precision without wasting precious computer time.

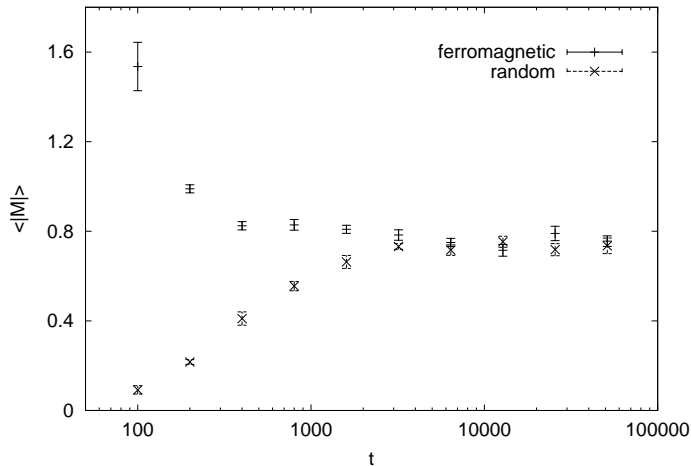


FIG. 1. Plot of magnetization per spin for a system of  $256$  Mn spins at  $T = 0.01$  as a function of time. The upper curve starts from ferromagnetic spin configuration, while the lower one from random configuration.

To determine the critical temperature in the model, we look, in particular, at the following dimensionless quantity widely used in spin systems [5]:

$$g(L) = \frac{1}{2} \left\{ 5 - 3 \frac{\langle |M|^4 \rangle}{\langle |M|^2 \rangle^2} \right\}, \quad (4)$$

for system of various sizes (numbers of Mn and electron spins) at different temperatures. The coefficients in the above equation have been chosen so that  $g(L) = 1$  at  $T = 0$ , and  $0$  as  $T \rightarrow \infty$ . In Fig. 2 we plot  $g(L)$  as a function of temperature  $T$ , for different number of Mn

spins. At large  $T$ ,  $g(L)$  decreases with number of Mn spins, or system size, while at low  $T$ , it increases with system size. The curves seem to cross around  $T = 0.014$ , at which  $g(L)$  is independent of  $L$ . We identify the crossing point as the transition temperature  $T_c$ , as suggested by finite size scaling theory.

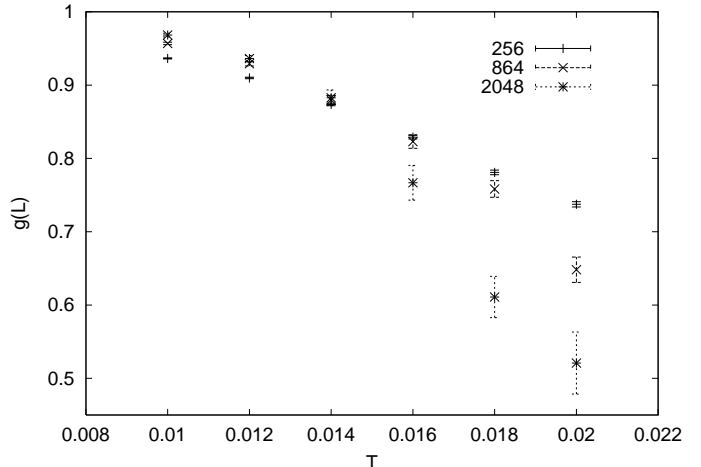


FIG. 2. Plot of  $g(L)$  for system of  $256$ ,  $864$ , and  $2048$  Mn spins at different temperatures around  $T_c = 0.014$ .

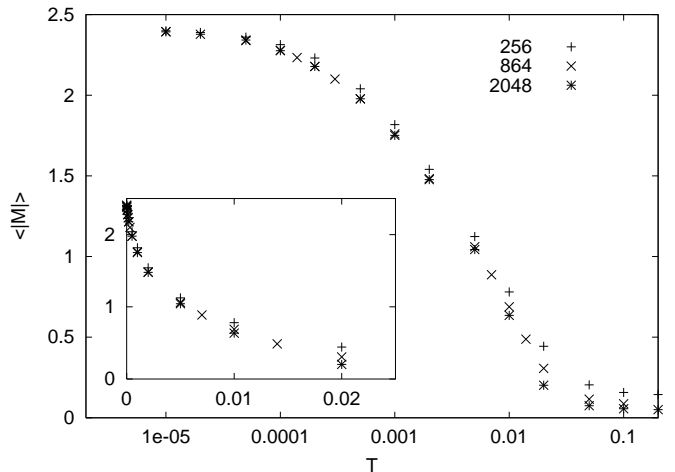


FIG. 3. Magnetization per spin versus temperature for system of  $864$  and  $2048$  Mn spins.

In Fig. 3 we plot the magnetization per spin at different temperatures for systems of  $864$  and  $2048$  Mn spins. Plotted on a logarithmic temperature scale, the magnetization curves look similar to what we observe in a typical ferromagnet on a linear plot. On a linear plot, however, it is seen that  $\langle |M| \rangle$  does not saturate even down to  $T_c/5$ . This can be understood as follows. The driving force behind the ferromagnetic transition is the ordering of Mn spins around each localized carrier into magnetic polarons. The radius of the polaron surrounding a dopant ion can therefore be estimated by equalizing the exchange energy at such distance to the ambient

temperature. For localized wavefunctions (in particular of the hydrogenic form), therefore, the radius of a polaron increases logarithmically with inverse temperature,  $r_T \sim (a_B/2) \ln(J_0 s T)$ . At a certain  $T$ , the radius of polarons grows large enough so that polarons percolate into a macroscopic ferromagnetic cluster, whose formation signals the transition,  $T_c$ . However, since the percolating cluster does not contain a majority of the spins until temperatures which are exponentially lower than  $T_c$ , most Mn spins remain free even in the ferromagnetic phase. It is these uncoupled spins which give rise to the slow saturation of magnetization at low  $T$ , and to the giant susceptibility peak below. The magnetization appears to approach the saturation value linearly at low  $T$ , within the precision of our simulation.

Figure 4 shows the plot of magnetic susceptibility as a function of  $T$  for different system sizes. Susceptibility increases dramatically when approaching the critical temperature  $T_c = 0.014$ , at which it diverges in the thermodynamic limit. Remarkably, there exists a huge peak at  $T = T_p$  two orders of magnitude below  $T_c$ , which appears to be  $L$ -independent for large enough lattices. Further analysis shows the peak at  $T_p$  is associated with single spin excitations of those Mn spins far away from any of the bound electrons.

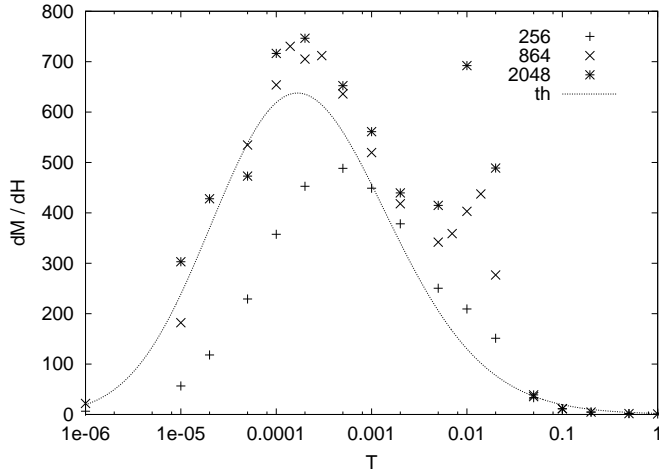


FIG. 4. Plot of susceptibility versus temperature  $T$  for systems of various number of Mn spins. Solid curve is the estimate of the contributions from manganese spins outside the percolating polaron cluster.

Well below  $T_c$ , it is convenient to view the system as a cluster of percolating polarons with a large number of Mn ions outside the cluster, which are interacting weakly with distant electron spins. Modeling the polarons as rigid shells of radius  $r_T$ , the number of Mn ions outside the polaron cluster can be estimated:

$$N_T = N_M P(r_T) = N_M e^{-4\pi\rho_c r_T^3/3}, \quad (5)$$

where  $N_M$  is the total number of Mn ions and  $\rho_c$  the doping density.  $P(r)$  is the probability of a magnetic ion having no bound electrons within distance  $r$ . Since

each of these Mn spins contributes  $S^2/3T$  to susceptibility in low temperature limit, the total susceptibility can be written as:

$$\chi_{\text{total}} = \frac{N_M S^2}{3T} e^{-4\pi\rho_c r_T^3/3}, \quad (6)$$

which fits the susceptibility peak in the simulation results reasonably well as shown in Fig. 4. Since finite system size prohibits the existence of manganese spins very far from any electron spins, the susceptibility peak at lower temperature is suppressed in small systems. Such an effect can be seen in the smallest system (256 Mn spins) in our simulation.

In Fig. 5, we show the specific heat per spin as a function of  $T$ . Notably, the specific heat does not vanish at low  $T$ , approaching unity instead. This is not surprising for a classical Heisenberg spin model, since the low temperature behavior must obey the classical equipartition theorem. In order to mimic the quantum mechanical characteristics of Mn spins without carrying out a full quantum Monte Carlo simulation, we have adopted a discrete vector model, in which each Mn spin can be oriented only along one of the six [100] directions. Spin flips in the vector model cost a finite energy therefore are frozen at very low temperatures.

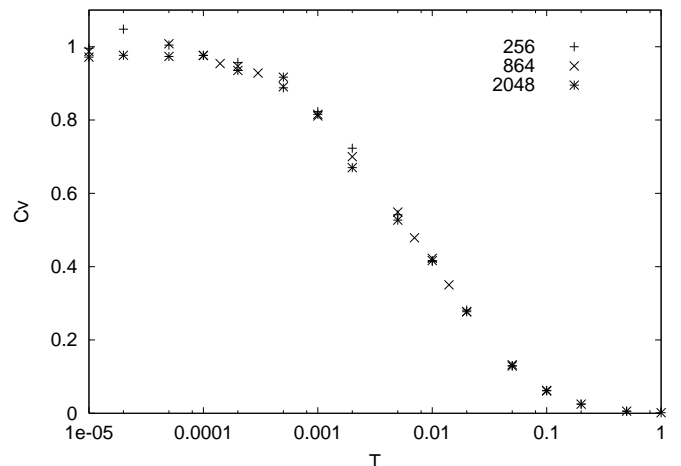


FIG. 5. Plot of  $Cv$  versus temperature in the classical Heisenberg spin model.

Results for a 12-state vector model has been investigated in more detail and published elsewhere [7]. In the two discrete spin models, the equilibration of a system, especially starting with random initial configurations, becomes extremely slow at low temperatures with single spin flips, when energy change associated with such a flip becomes exponentially larger than the temperature. In fact, most of the samples are frozen in metastable states. A cluster algorithm, which is capable of updating large number of spins (within a polaron or a percolating polaron cluster) in a single step, has been introduced to speed up the equilibration [7]. The algorithm has been

found to attain convergence at low temperatures, especially in small samples.

The introduction of discrete spin models leads to qualitatively similar magnetization and susceptibility curves. The magnetic susceptibility shows a peak two orders of magnitude below  $T_c$ . Yet, the discreteness of energy levels simulates the quantization of spin energy levels as desired. Figure 6 shows the plot of specific heat of a system of 864 Mn spins at different temperatures in the 6-vector model. As a result of discrete symmetry, specific heat per spin drops to zero in low temperature limit. Following a similar argument as for the susceptibility, one can show [6]

$$C_v \sim \rho_c a_B r_T^2 e^{-4\pi\rho_c r_T^3/3}, \quad (7)$$

which fits the simulation results very well.

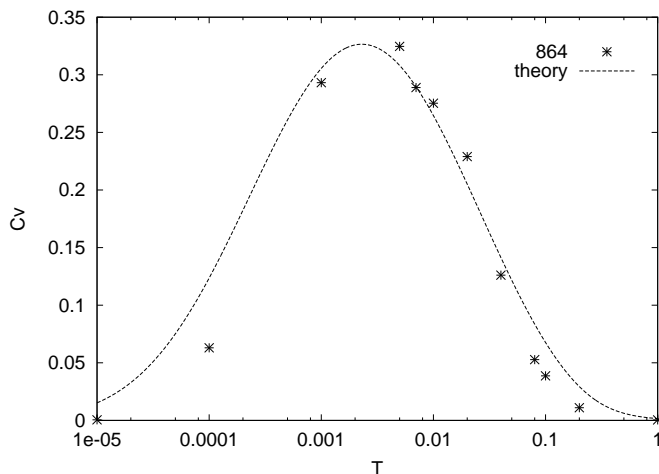


FIG. 6.  $C_v$  at different temperatures for a system of 864 Mn spins in the discrete vector model. The solid line is the theoretical estimate.

The simulations reported above were for a low concentration of magnetic ions and a low concentration of dopants with a ratio such that the interaction between Mn spins and between carrier spins can be neglected, and further, the dominant carrier-Mn interaction can be well estimated through the isolated carrier wavefunction. However, as a consequence, the transition temperature is very low which makes relevant experimental observations almost impossible. We can raise the temperature range of interest by increasing the concentration of dopants ( $n_d$ ); however, working within a pure spin model restricts the carrier density to lie below the metal-insulator transition (MIT) density so the system stays insulating. Increasing both the Mn concentration and dopant concentration by a factor of 2 gets us close to the MIT ( $n_d^{1/3} a_B = 0.25$ ). Figure 7 shows the susceptibility for system of 512 and 1728 Mn spins as a function of  $T$ . Both  $T_c$  and  $T_p$  increase significantly, still leaving roughly one order of magnitude difference between the two temperatures. There is a decrease in the height of the low temperature peak, because

increasing the dopant concentration reduces the number of weakly coupled Mn spins. Our theoretical estimate again fits these results very well, which implies that the main contribution of the low temperature peak comes from such isolated Mn spins.

While these simulations were done for the insulating regime, we expect that the onset of metallicity, especially just above the MIT, will not change qualitatively the unusual aspects of the magnetic behavior of doped DMS. In fact, unusual magnetization curves have been reported in experiments on metallic  $Ga_{1-x}Mn_xAs$ , a III-V DMS, where Mn contributes both a localized magnetic moment and a carrier (but the system appears to be heavily compensated, so the carrier density is only about 10% of the Mn density) [8]. These effects, arising from disorder in the Mn and dopant positions, have been left out in recent models [9,10] that have appeared in the literature since the completion of this work. Preliminary results of a numerical study of metallic doped III-V DMS [11] taking into account the disorder in the Mn positions shows that qualitative effects seen in this study remain important at the densities well beyond the MIT.

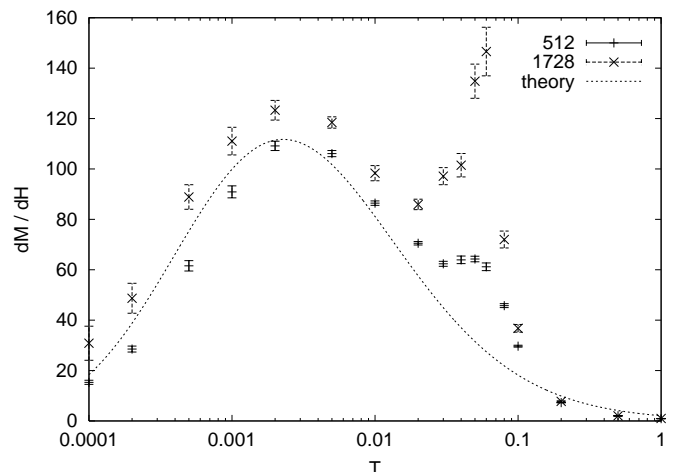


FIG. 7. Plot of susceptibility versus temperature  $T$  for systems of various number of Mn spins near the metal-insulator transition concentration. Solid curve is the estimate of the contributions from Mn spins outside the percolating polaron cluster.

In summary, we have demonstrated via a Monte Carlo study, a ferromagnetic transition in doped, diluted magnetic semiconductors in the low doping (insulating) regime. Though the model studied has no frustration, it has a very high degree of disorder, characterized by a wide distribution of exchange couplings. As a result, the system exhibits very unusual properties, such as thermodynamic properties (e.g., magnetization, magnetic susceptibility, specific heat) which are very different from homogeneous systems. In particular, standard expansions used for homogeneous systems - critical fluctuations around the transition temperature, or spin wave expansions around the ordered state ( $T = 0$ ), do very poorly

in describing the thermodynamics over most of the phase diagram. There is considerable thermodynamic entropy down to very low temperatures, leading to an unusual peak in the magnetic susceptibility and specific heat at a temperature well below the transition temperature. Our simulations demonstrate the necessity of incorporating the discrete nature of the quantum Heisenberg spins (despite the ferromagnetic nature of the ordered state), and the possibility of unusual thermodynamics in the  $T \rightarrow 0$  limit also. Some of the qualitative features are expected to survive in the case of metallic doped DMS as well.

This research was supported by NSF DMR-9809483.

- 
- [1] For reviews, see *Semiconductors and Semimetals*, edited by J. K. Furdyna and J. Kossut (Academic, San Diego, 1988), Vol. 25, P. 413.
  - [2] P. A. Wolff, in *Semimagnetic and Diluted Magnetic Semiconductors*, ed. M. Averous and B. Balkanski (Plenum, New York, 1991).
  - [3] J. Z. Liu, G. Lewen, P. Becla, and P. A. Wolff, *Bull. Am. Phys. Soc.* **39**, 402 (1994).
  - [4] P. A. Wolff, R. N. Bhatt, and A. C. Durst, *J. Appl. Phys.* **79**, 5196 (1996).
  - [5] K. Binder and A. P. Young, *Rev. Mod. Phys.* **58**, 801 (1986).
  - [6] R. N. Bhatt, *Bull. Am. Phys. Soc.* **44**, 714 (1999).
  - [7] For more details on a similar 12-vertex model, see R. N. Bhatt and X. Wan, *Int. J. Mod. Phys. C* **10**, 1459 (1999).
  - [8] B. Beschoten, P. A. Crowell, I. Malajovich, D. D. Awschalom, F. Matsukura, A. Shen, and H. Ohno, *Phys. Rev. Lett.* **83**, 3073 (1999).
  - [9] J. Konig, H. H. Lin, and A. H. MacDonald, *Phys. Rev. Lett.* **84**, 5628 (2000).
  - [10] T. Dietl, H. Ohno, F. Matsukura, J. Cibert, and D. Ferrand, *Science* **287**, 1019 (2000).
  - [11] M. Berciu and R. N. Bhatt, unpublished.